

Cu/Zn disorder in stoichiometric $\text{Cu}_2\text{ZnSn}(\text{S}_{1-x}\text{Se}_x)_4$ semiconductors: a complementary neutron and anomalous X-ray diffraction study

Galina Gurieva^{1*}, Daniel M. Töbrens¹, Sergiu Levenco², Thomas Unold¹ and Susan Schorr^{1,3}

¹ Helmholtz Zentrum Berlin für Materialien und Energie GmbH, Hahn-Meitner-Platz 1, D-14109 Berlin, Germany

² Felix-Bloch-Institut für Festkörperphysik, Universität Leipzig, Linnéstraße 5, 04103 Leipzig, Germany

³ Free University Berlin, Institute of Geological Sciences, Malteserstr. 74-100, Berlin, Germany

* Corresponding author galina.gurieva@helmholtz-berlin.de

Abstract

The quaternary compound semiconductor $\text{Cu}_2\text{ZnSn}(\text{S}_{1-x}\text{Se}_x)_4$ (CZTSSe) which crystallizes in the kesterite-type structure, is a promising material to be used as p-type absorber layer in thin film solar cell applications based on earth abundant elements. The absorber band tailing caused by an exceptionally high Cu/Zn disorder is believed to be one of the reasons for the limited open-circuit voltage in CZTSSe-based photovoltaic devices. This work is an experimental study of the Cu/Zn disorder in a unique set of single phase, stoichiometric CZTSSe mixed crystals, synthesized by solid state reaction, by means of neutron powder diffraction and anomalous X-ray powder diffraction. The existence of Cu/Zn disorder was revealed as the only intrinsic point defect in these mixed crystals within the detection limits of our measurements. The order parameter Q was calculated on the basis of the occurring Cu_{Zn} and Zn_{Cu} anti site defects causing the Cu/Zn disorder. Variations of the order parameter with anion composition and the effect on the optoelectronic properties of the partial substitution of Se with S in $\text{Cu}_2\text{ZnSn}(\text{S}_{1-x}\text{Se}_x)_4$ was elaborated.

Keywords: CZTSSe, Cu/Zn disorder, neutron diffraction, anomalous X-ray diffraction, photoluminescence

Introduction

Recently quaternary chalcogenides have gained a lot of attention, especially compound semiconductors of the $\text{Cu}_2\text{ZnSn}(\text{S}_{1-x}\text{Se}_x)_4$ solid solution series, which consist mostly of earth abundant and non-toxic elements. These kesterite-type compounds are promising low cost alternative absorber materials for thin film solar cells due to having properties suitable for photovoltaic applications: p-type semiconductor behavior, direct band-gap between 1.0-1.5 eV and absorption coefficient $> 10^4 \text{ cm}^{-1}$ [1, 2]. The best photovoltaic performance of kesterite-based thin film solar cells were obtained with Se-rich $\text{Cu}_2\text{ZnSn}(\text{S},\text{Se})_4$ (CZTSSe) absorbers with conversion efficiency of 12.6% [3]. However, a common phenomenon observed in such devices is a low open circuit voltage with respect to the band gap, evidencing the existence of a number of challenges that must still be faced in order to achieve high quality, efficient solar cells. The absorber band tailing caused by the exceptionally high density of Cu_{Zn} and Zn_{Cu} anti-sites causing Cu/Zn disorder [4] is believed to be one of the reasons for the limited open-circuit voltage in CZTSSe-based devices [5]. An order-disorder phase transition was reported for $\text{Cu}_2\text{ZnSnS}_4$ (CZTS) at $T= 260^\circ\text{C}$ [6], in $\text{Cu}_2\text{ZnSnSe}_4$ (CZTSe) this transition occurs at $T=200^\circ\text{C}$ [7]. In these and other studies the distribution of the cations Cu^{1+} and Zn^{2+} in the kesterite-type crystal structure has been approached in various ways. The decrease of Cu/Zn disorder at temperatures below the

order-disorder transition temperature was mainly deduced indirectly: by anomalous lattice parameter expansion [8], Raman spectroscopy and spectrophotometry [6], electro-reflectance [9], and from kinetics simulations [10].

Numerous studies published in literature are devoted to the end members of the CZTSSe solid solution, and in most of the cases thin films are studied. Thin film absorber layers are usually inhomogeneous, with an off-stoichiometric absorber composition and with secondary phases being present. To separate the Cu_{Zn} and Zn_{Cu} anti-site point defects which cause the Cu/Zn disorder from point defects correlated to the off-stoichiometric composition of the kesterite-type semiconductor (e. g. vacancies, interstitials and anti-sites) is a very complex problem. Only few experimental methods allow tackling Cu/Zn disorder directly, most promising among them being neutron and anomalous X-ray diffraction. Cu^{1+} and Zn^{2+} are isoelectronic cations and thus have essentially the same scattering factor for X-rays. Thus they cannot be distinguished by conventional X-ray diffraction. To overcome this problem, neutron diffraction has been used to study the crystal structure, structural disorder and point defects in stoichiometric CZTS, CZTSe, off-stoichiometric CZTSe as well as $\text{Cu}_2\text{ZnGeSe}_4$ (CZGSe) [4, 11-15]. The possibility to use anomalous synchrotron X-ray diffraction had been exploited sporadically [16] until recently when a new method for data evaluation was developed [17]. In the present work we applied both, neutron and anomalous X-ray diffraction, in order to obtain the distribution of Cu and Zn in the crystal structure of CZTSSe to determine the concentration of Cu_{Zn} and Zn_{Cu} anti site defects in a unique set of single phase stoichiometric CZTSSe mixed crystals. The method applied allows the direct determination of the degree of disorder, described by the order parameter Q [7].

Experimental

Powder samples covering the complete $\text{Cu}_2\text{ZnSn}(\text{S}_{1-x}\text{Se}_x)_4$ solid solution series (table 1) were synthesized by solid state reaction of the pure elements, which is a proven reliable method for a systematic approach [13, 14, 18, 19]. Weighted stoichiometric mixtures of elemental zinc (5N), copper (5N), tin (5N), sulfur (5N) and selenium (6N) were placed in a pyrolytic graphite boat and sealed in evacuated quartz ampoules. Each tube was placed in a one-zone furnace and heated at a rate of 10 K/h, with intermediate temperature steps of 250°C and 450°C held for 48h each, up to a final temperature, which varied between 700°C (for Se end member) and 800°C (for pure S end member) depending on the S/(S+Se) ratio. After holding the final temperature for 240 h the samples were cooled to room temperature dynamically by switching off the furnace. A homogenization step (grinding in an agate mortar and pressing pellets) was followed by final annealing of each pellet in an evacuated silica tube in a one zone furnace at the same final temperature as before for 240 h, again followed by dynamic cooling. Several attempts were performed for synthesise stoichiometric sulphur-rich mixed crystals but with only limited success. Selenium-rich mixed crystals were obtained from the first trial.

Back scatter electron (BSE) micrographs (Figure 1) revealed already the inhomogeneity of S-rich mixed crystals (see figure 1a) and the homogeneity of the Se-rich samples (see figure 1b). Wavelength dispersive X-ray spectroscopy (WDX) has been performed to determine the phase content and chemical composition of the synthesized material using an electron microprobe analysis system. In order to obtain reliable results from the WDX measurements, the system was calibrated using NIST elemental standards. High accuracy of the compositional parameters was achieved by averaging over 20 local measured points within one grain and averaging over more than 30 grains of the CZTSSe phase to achieve the chemical composition of the main phase. In case of secondary phases being present additional grains containing secondary phase were measured in the same way. The complete overview of the obtained cation ratios and deduced chemical composition of the CZTSSe mixed crystals as well as a list of secondary phases (when present) is shown in Table 1. This compositional and phase analysis

revealed striking differences between Se-rich and S-rich mixed crystals. Se-rich mixed crystals form homogeneous, single phase CZTSSe with stoichiometric composition. In case of S-rich CZTSSe samples the obtained CZTSSe main phase shows an off-stoichiometric but homogeneous chemical composition and binary secondary phases are present. Only in the sample containing the CZTSSe phase with the highest sulfur content, no secondary phases could be observed. For all off-stoichiometric CZTSSe phases the off-stoichiometry type was determined from the cation ratios according to a procedure reported previously [13, 14, 18]. The cation ratio plot (figure 2) gives an overview of the synthesized CZTSSe mixed crystals.

Based on the results of the chemical analysis, the focus of the detailed structural investigation of the Cu/Zn disorder was restricted to the Se-rich stoichiometric CZTSSe mixed crystals. A detailed study of the single phase off-stoichiometric $\text{Cu}_2\text{ZnSn}(\text{S}_{1-x}\text{Se}_x)_4$ solid solution with $\text{Se}/(\text{S}+\text{Se}) = 0.48$ was published previously [19].

Neutron powder diffraction data were collected at the Berlin Research Reactor BER II at the Helmholtz-Zentrum Berlin für Materialien und Energie (HZB) using the fine resolution powder diffractometer FIREPOD (E9) ($\lambda = 1.798 \text{ \AA}$; ambient temperature) [20]. Data analysis was done by full pattern Rietveld refinement [21] using the FullProf Suite software package [22]. The kesterite type structure with Cu on Wyckoff position $2a:(0,0,0)$ and $2c:(0,\frac{1}{2},\frac{1}{4})$, Zn on $2d:(0, \frac{1}{2},\frac{3}{4})$, Sn on $2b:(\frac{1}{2}, \frac{1}{2},0)$ and S and Se on $8g:(x,y,z)$ was used as structural model in the refinement [11]. The refinement of site occupancy factors (SOF) was done without any chemical constraints. An example of the neutron diffraction pattern and corresponding Rietveld analysis is shown in Figure 3, significant results are listed in table 2.

Anomalous synchrotron powder diffraction data (AXRPD) at ambient conditions were collected at the diffraction end station of the beamline KMC-2 [23] at the synchrotron radiation source BESSY II (HZB). In order to make use of changes in the energy-dependent parts f' and f'' of the atomic scattering factor f with $f = f_0(2\theta) + f'(\lambda) + i \cdot f''(\lambda)$, of both Cu and Zn, high quality diffraction data were collected for each sample at multiple radiation energies below the K-absorption edges of both Cu and Zn (8919, 8955, 8969, 8974 eV and 9599, 9635, 9649, 9654 eV, respectively), where anomalous effects are strong, and at energies far away of these edges (8048 and 9376 eV). Previously established measurement conditions and data treatment procedures were used (for details see [17]). The obtained diffraction data have been evaluated by the Rietveld refinement. Occupation factors of the Wyckoff sites $2a$, $2c$, and $2d$ of the Kesterite type structure model have been refined or each individual pattern similar to the analysis of neutron diffraction data. Plotting these site occupation factors for each CZTSSe mixed crystal as a function of the atomic scattering factor ratio allowed determination of the occupation factors for both copper and zinc sites (table 3) from linear fits [for details see 17].

A thorough characterization of CZTSSe mixed crystals (powder and polycrystalline thin films) by Raman spectroscopy was presented in [24], including a detailed deconvolution of the spectra using the Lorentzian peak shape function. Additionally, the possible presence of ZnSe as secondary phase was excluded by Raman scattering measurements using a 457.9 nm excitation wavelength, which corresponds to the resonant excitation condition for this binary compound. A simple and non-destructive optical methodology for the quantitative measurement of $[\text{S}]/([\text{S}] + [\text{Se}])$ anion composition in $\text{Cu}_2\text{ZnSn}(\text{S}_x\text{Se}_{1-x})_4$ solid solutions by means of Raman spectroscopy in the whole S–Se range of compositions has been developed based on this solid solution series as shown in [24]. It has to be noted that in light of the results presented here, this relation has to be considered a function of the integral (total) composition of the material. It remains valid even in S-rich samples, where secondary phases are present and the CZTSSe phase is invariably off-stoichiometric.

Photoluminescence (PL) measurements were performed at ambient temperature using a 660 nm diode laser as excitation source. The PL signals are detected with a 1/2m grating monochromator equipped with a liquid N₂ cooled InGaAs array type detector.

Results and discussion

The structural parameters of the CZTSSe mixed crystals obtained by Rietveld analysis of neutron diffraction data are listed in table 2. Final resulting cation site occupancy factors (SOF) determined from both, neutron diffraction and AXRPD are given in table 3.

The average neutron scattering length analysis method [25] was applied to determine the distribution of the cations Cu^+ , Zn^{2+} and Sn^{4+} on the four structural sites of the kesterite type structure (2a, 2b, 2c and 2d). The experimental average neutron scattering lengths were calculated according to eqs. 1 using the cation site occupancy values SOF_{2a} , SOF_{2c} , SOF_{2d} and SOF_{2b} determined by Rietveld analysis of neutron diffraction data

$$\begin{aligned}\bar{b}_{2a}(\text{exp}) &= \text{SOF}_{2a} \cdot b_{\text{Cu}} \\ \bar{b}_{2c}(\text{exp}) &= \text{SOF}_{2c} \cdot b_{\text{Cu}} \\ \bar{b}_{2b}(\text{exp}) &= \text{SOF}_{2d} \cdot b_{\text{Zn}} \\ \bar{b}_{2d}(\text{exp}) &= \text{SOF}_{2b} \cdot b_{\text{Sn}}\end{aligned}\quad (1)$$

Comparing these values with the neutron scattering lengths of copper, zinc and tin (b_{Cu} , b_{Zn} , b_{Sn}) it becomes obvious that the average neutron scattering length of the copper site 2a ($\bar{b}_{2a}(\text{exp})$) in all of the CZTSSe mixed crystals studied is the same as the scattering length of copper (within an experimental uncertainty). The same situation can be found for the 2b site relating to tin occupation. This is a strong indication that both of these sites are fully occupied by the element expected according to the kesterite-type structure: Cu in case of the Wyckoff position 2a and Sn in case of the 2b site. The situation is different for the cation sites 2c and 2d. The average neutron scattering length of the 2c site ($\bar{b}_{2c}(\text{exp})$), which according to the kesterite-type structure should be fully occupied by copper, is decreased in comparison with the neutron scattering length of copper, while the average neutron scattering length of the 2d site ($\bar{b}_{2d}(\text{exp})$), which in the kesterite-type structure is fully occupied by zinc, is increased in comparison to the neutron scattering length of zinc (see Figure 4).

Taking into account the experimentally determined total amounts of each element, as obtained by WDX analysis, and assuming that all four cation sites are fully occupied, the respective cation occupancy of the sites can be derived with high reliability. The average neutron scattering length of site 2c indicates, that this copper site is partly occupied by zinc and/or tin respectively, decreasing the experimental average neutron scattering length. On the other hand, the experimental average neutron scattering length of the zinc site 2d indicates partial occupation by copper and/or tin, increasing the average neutron scattering length. However, for both sites the presence of Sn on the sites 2c and 2d can be excluded due to the fact that the site 2b is fully occupied by Sn and the elemental analysis of the CZTSSe mixed crystals does not show a Sn excess present. As a result of the average neutron scattering length analysis, concerning the sites 2c and 2d the only possible point defects are Cu_{Zn} and Zn_{Cu} anti-site defects, moreover, those anti-sites are present in the same amounts ($2c:\text{Cu}_{\text{Zn}} = 2d:\text{Zn}_{\text{Cu}}$). This type of Cu/Zn disorder, effectively exchanging Cu and Zn cations between the 2c and 2d Wyckoff positions, has been found to be the only defect present within all of studies the stoichiometric Se-rich CZTSSe mixed crystals (see Figure 5).

An independent second determination of the site occupancy factors has been derived from combined analysis of the anomalous X-ray diffraction data [17]. The site occupancy parameter of the 2b site had to be fixed to full occupation by Sn, as stipulated from chemical analysis and neutron diffraction data

analysis, as correlation with the other site occupancies would be too high otherwise [7, 17]. Even so, uncertainties are still higher than those determined by neutron diffraction. The obtained site occupancy factors (figure 6, table 3) are proven against the overall chemical composition and full site occupancy. Results are in all cases in agreement within uncertainties with those from the neutron data analysis.

Using the site occupancy factors the order parameter of Cu/Zn disorder can be calculated. This order parameter Q is defined in such a way that $Q = 0$ for complete disorder and $Q = 1$ for order. In literature different approaches can be found [7, 10, 26] depending on whether the copper site $2a$ is included and how vacancies are treated. For the kesterite-type CZTSSe phases studied here, where the site $2a$ is completely occupied by copper, the approach discussed in [7] was used. It takes into consideration that to make the order parameter useful in symmetry-based descriptions of the phase transition, e.g. Landau theory [27], Q should depend only on the parameters, whose symmetry is broken by the phase transition. In this case this is the occupation of the $2c$ and $2d$ sites. Thus eq.2 was adapted from [7]:

$$Q = \frac{[Cu_{2c}+Zn_{2d}]-[Zn_{2c}+Cu_{2d}]}{[Cu_{2c}+Zn_{2d}]+[Zn_{2c}+Cu_{2d}]}, \quad (2)$$

The order parameter Q was calculated for both sets of data obtained (neutron diffraction as well as anomalous X-ray diffraction), and compared in order to find the dependency of Cu/Zn disorder from the Se/(S+Se) ratio. The result is presented in figure 7.

While uncertainties are too high to allow a discussion of fine details of the disorder, some features are unambiguous. A notable trend towards higher Cu/Zn-disorder (i. e. lower values of the order parameter Q) in CZTSSe Kesterite-type phases with higher sulfur content can be observed. This might be a result of the higher anion disorder in these materials. It can be expected that S-Se-disorder translates to disorder of other structural parameters at least to some degree. If this mechanism is indeed in play here, the trend can be expected to invert direction in the sulfur-rich part of the solution series. Cation disorder should be lowest in the pure endmembers, where anion disorder does not exist. However, the absence of stoichiometric S-rich CZTSSe complicates the situation, so that this hypothesis currently cannot be tested experimentally. The correlation between order parameter Q and Se/(S+Se) ratio (figure 7) is rather weak. In particular, neither the neutron nor the APXRD analysis gives the pure CZTSe phase as the one with the lowest disorder, but the sample with Se/(S+Se) ratio of 0.9. This is the only sample for which $Q > 0.5$ was observed, the exception in the series tending towards ordered kesterite instead of disordered.

In all samples, even in the one with the lowest degree of disorder, the concentration of Cu_{Zn} and Zn_{Cu} anti sites correlated to Cu/Zn disorder is very high, in the order of 10^{20} - 10^{21} cm^{-3} . Significant influence of such a high defect concentration on the electronic properties of the compounds can be expected. Figure 8a shows the photoluminescence (PL) spectra of the Se-rich CZTSSe Kesterite-type solid solutions as a function of the Se/(S+Se) content. A weak broad PL band emission with the full width at the half maximum (FWHM) of about 0.15 eV is shifted to low photon energies with the increase of the Se content. The PL emission maximum (PL_{max}) associated with the PL transition energy is shown as function of the Se content (Figure 8b).

The band gap transition energy can be calculated theoretically [29] according to $E_g(x)=(1-x)*1.5+x*0.96+0.1*x(1-x)$, where x is the Se content. A dependence of the band gap energy $E_g(x)$ on the chemical composition has also been supported by experimental data [30]. The observed PL_{max} values of the studied Se-rich CZTSSe mixed crystals are significant smaller (by 0.05 – 0.1 eV) than the theoretically calculated E_g values [29], with an exception of the CZTSSe phase with the highest Se

content ($x=0.9$) (see figure 8b). Moreover the observed difference between PL_{max} and E_g is decreased with increasing Se content in the Kesterite-type mixed crystals. However, the Se-rich CZTSSe samples have different Cu/Zn disorder, which in turn influences the E_g and PL_{max} [7, 9, 10]. To account the effect of increasing Cu/Zn disorder with decreasing Se content in CZTSSe mixed crystals, E_g values obtained in polycrystalline CZTSSe thin films (with $Se/(S+Se)=0.92$ and 1.0) which have been thermally treated to show different degrees of disorder (named “ordered” and “disordered”) [9, 10] were taken into account. The difference in E_g between “disordered” and “ordered” CZTSSe in the thin films is 0.12 eV. Based on these E_g the curves, linear extrapolated to S-rich compositions, have been added in figure 9b. In this way we can show that CZTSSe mixed crystals with lower Cu/Zn disorder (CZTSe, Se90 and Se80) show PL transition energies (PL_{max}) smaller at least by 90 meV than the band gap energy of “ordered” kesterite-type CZTSSe and could be attributed to a band-to-acceptor type PL transition [28]. In contrast the CZTSSe mixed crystals with lower Q-parameter (Se60 and Se70) exhibit PL transition energies close to the band gap of “disordered” CZTSSe and could be assigned to a band-to-band type transition [9, 10].

Summary and conclusions

The unique series of single phase, stoichiometric mixed crystals within the $Cu_2ZnSn(S_{1-x}Se_x)_4$ solid solution series (powder samples with $x=0.5..1$), grown by solid state reaction, have been investigated by means of neutron and anomalous X-ray diffraction. The method of the average neutron scattering length analysis was applied to establish a cation distribution model which was used to reveal the occurring intrinsic point defects in the kesterite-type material. The cation distribution resulting from the anomalous X-ray diffraction data analysis are in very good agreement with those obtained from the neutron data analysis. The only point defect present within all of the stoichiometric CZTSSe mixed crystals was found to be Cu_{Zn} and Zn_{Cu} anti sites causing Cu/Zn disorder in the lattice planes at $z=1/4$ and $3/4$: the exchange of Cu and Zn cations between the $2c$ and $2d$ Wyckoff positions in equal amounts. A notable trend towards higher Cu/Zn-disorder in CZTSSe Kesterite-type phases with higher S content was observed. The room temperature PL measurements revealed a strong effect of the anion composition and order parameter on the electronic properties of studied CZTSSe mixed crystals.

Acknowledgements

The research leading to the presented results has been partially supported by the STARCELL project as well as INFINITE-CELL project. These projects have received funding from the European Union’s Horizon 2020 research and innovation programme under the Marie Skłodowska-Curie grant agreements No 720907 and 777968 respectively.

We thank HZB for the allocation of neutron and anomalous X-ray diffraction beamtimes.

References

- [1] J.M. Raulot, C. Domain, J.F. Guillemoles, Ab initio investigation of potential indium and gallium free chalcopyrite compounds for photovoltaic application, *Journal of Physics and Chemistry of Solids*, 66 (2005) 2019-2023.

- [2] P.A. Fernandes, P.M.P. Salomé, A.F. da Cunha, $\text{Cu}_x\text{SnS}_{x+1}$ ($x = 2, 3$) thin films grown by sulfurization of metallic precursors deposited by dc magnetron sputtering, *physica status solidi (c)*, 7 (2010) 901-904.
- [3] W. Wang, M.T. Winkler, O. Gunawan, T. Gokmen, T. Todorov, Y. Zhu, D. B. Mitzi, Device Characteristics of CZTSSe Thin-Film Solar Cells with 12.6% Efficiency, *Adv. Energy Mater.*, (2014), 4: 1301465.
- [4] S. Schorr, The crystal structure of kesterite type compounds: A neutron and X-ray diffraction study, *Solar Energy Materials and Solar Cells*, 95 (6), (2011), 1482.
- [5] X. Liu, Y. Feng, H. Cui, F. Liu, X. Hao, G. Conibeer, D.B. Mitzi, and M. Green, The current status and future prospects of kesterite solar cells: a brief review, *Prog. Photovolt: Res. Appl.*, 24, (2016), 879–898.
- [6] J. J. S. Scragg, L. Choubrac, A. Lafond, T. Ericson, and C. Platzer-Björkman, A low-temperature order-disorder transition in $\text{Cu}_2\text{ZnSnS}_4$ thin films, *Appl. Phys. Lett.*, 104, 4, (2014) 041911.
- [7] D. M. Többens, G. Gurieva, S. Levchenko, T. Unold, S. Schorr, Temperature dependency of Cu/Zn ordering in CZTSe kesterites determined by anomalous diffraction, *Physica Status Solidi B* 253 (2016), 1890-1897
- [8] S. Schorr, G. Gonzalez-Aviles, In-situ investigation of the structural phase transition in kesterite, *Phys. Stat. Solidi A*, 206, 5, (2009), 1054.
- [9] C. Krammer, C. Huber, C. Zimmermann, M. Lang, T. Schnabel, T. Abzieher, E. Ahlswede, H. Kalt, & M. Hetterich, Reversible order-disorder related band gap changes in $\text{Cu}_2\text{ZnSn}(\text{S},\text{Se})_4$ via post-annealing of solar cells measured by electroreflectance, *Applied Physics Letters*, 105, (2014), 262104.
- [10] G. Rey, A. Redinger, J. Sendler, T. P. Weiss, M. Thevenin, M. Guennou, B. El Adib. & S. Siebentritt, The band gap of $\text{Cu}_2\text{ZnSnSe}_4$: Effect of order-disorder, *Applied Physics Letters*, 105, (2014), 112106.
- [11] S. Schorr, H.-J. Höbner, M. Tovar, A neutron diffraction study of the stannite-kesterite solid solution series, *Europ. Jour. Mineral.*, 19, (2007), 65 – 73.
- [12] S. Siebentritt, S. Schorr, Kesterites—a challenging material for solar cells, *Progress in Photovoltaics: Research and Applications*, 20(5), (2012), 512.
- [13] G. Gurieva, L.E. Valle Rios, A. Franz, P. Whitfield, S. Schorr, Intrinsic point defects in off-stoichiometric $\text{Cu}_2\text{ZnSnSe}_4$: A neutron diffraction study, *Journal of Applied Physics* 123 (2018), 161519/1-12
- [14] R. Gunder, J. Márquez Prieto, G. Gurieva, T. Unold, S. Schorr, Structural characterization of off-stoichiometric kesterite-type $\text{Cu}_2\text{ZnGeSe}_4$ compound semiconductors: from cation distribution to intrinsic point defect density, *CrystEngComm*, 20, (2018), 1491.
- [15] G. Gurieva, D. M. Toebbens, M. Ya. Valakh, S. Schorr, Cu-Zn disorder in $\text{Cu}_2\text{ZnGeSe}_4$: A complementary neutron diffraction and Raman spectroscopy study, *Journal of Physics and Chemistry of Solids* 99 (2016), 100-104
- [16] A. Lafond, L. Choubrac, C. Guillot-Deudon, P. Deniard, S. Jobic, Crystal structures of photovoltaic chalcogenides, an intricate puzzle to solve: the cases of CIGSe and CZTS materials, *Z. Anorg. Allg. Chem.*, 638, (2012), 2571–2577.

- [17] D.M. Töbrens, R. Gunder; G. Gurieva, J. Marquardt, K. Neldner, L.E. Valle-Rios, S. Zander, S. Schorr, Quantitative anomalous powder diffraction analysis of cation disorder in kesterite semiconductors, *Powder Diffraction* 31 (2016), 168-175
- [18] L. E. Valle Rios, K. Neldner, G. Gurieva and S. Schorr, Existence of off-stoichiometric single phase kesterite, *J. Alloys Comp.* 657, (2016), 408.
- [19] G. Gurieva, M. Dimitrievska, S. Zander, A. Pérez-Rodríguez, V. Izquierdo-Roca, S. Schorr, Structural characterisation of $\text{Cu}_{2.04}\text{Zn}_{0.91}\text{Sn}_{1.05}\text{S}_{2.08}\text{Se}_{1.92}$, *Phys. Stat. Sol. C*, 12, 6, (2015), 588.
- [20] Helmholtz-Zentrum Berlin für Materialien und Energie. E9: The Fine Resolution Powder Diffractometer (FIREPOD) at BER II. *Journal of large-scale research facilities*, 3, A103. (2017)
- [21] H.M. Rietveld, A profile refinement method for nuclear and magnetic structures, *J. Appl. Crystallogr.* 2, (1969), 65-71.
- [22] Juan Rodriguez-Carvajal and Thierry Roisnel, www.ill.eu/sites/fullprof/
- [23] Helmholtz-Zentrum Berlin für Materialien und Energie. KMC-2: an X-ray beamline with dedicated diffraction and XAS endstations at BESSY II. *Journal of large-scale research facilities*, 2, A49 (2016), doi: 10.17815/jlsrf-2-65
- [24] M. Dimitrievska, G. Gurieva, H. Xie, A. Carrete, A. Cabot, E. Saucedo, A. Pérez-Rodríguez, S. Schorr, V. Izquierdo-Roca, Raman scattering quantitative analysis of the anion chemical composition in kesterite $\text{Cu}_2\text{ZnSn}(\text{S}_x\text{Se}_{1-x})_4$ solid solutions, *Journal of Alloys and Compounds* 628 (2015), p. 464-470
- [25] S. Schorr, X-Ray and Neutron Diffraction on Materials for Thin-Film Solar Cells, in *Advanced Characterization Techniques for Thin Film Solar Cells*, T.K.a.U.R. D. Abou-Ras, Editor. 2011, Wiley-VCH Verlag GmbH & Co. KGaA. 347.
- [26] A.Ritscher, M. Hölzel, & M. Lerch, The order-disorder transition in $\text{Cu}_2\text{ZnSnS}_4$ — A neutron scattering investigation, *Journal of Solid State Chemistry* 238, (2016), 68 - 73.
- [27] J.-C. Toledano, & P.Toledano, (1987). *The Landau theory of phase transitions*. Singapore: World Scientific Publishing.
- [28] S. Levchenko, J. Just, A. Redinger, G. Larramona, S. Bourdais, G. Dennler, A. Jacob, T. Unold, Deep Defects in $\text{Cu}_2\text{ZnSn}(\text{S},\text{Se})_4$ Solar Cells with Varying Se Content, *Phys. Rev. Appl.*, 5 (2), (2016), 1–10.
- [29] S.Chen, A. Walsh, J.H. Yang, X.G. Gong, L. Sun, P.X. Yang, J.H. Chu, and S.H. Wei, Compositional dependence of structural and electronic properties of $\text{Cu}_2\text{ZnSn}(\text{S},\text{Se})_4$ alloys for thin film solar cells, *Physical Review B* 83, (2011), 125201.
- [30] J. He, L. Sun, S. Chen, Y. Chen, P. Yang, and J. Chu, Composition dependence of structure and optical properties of $\text{Cu}_2\text{ZnSn}(\text{S},\text{Se})_4$ solid solutions: An experimental study *J. Alloys Compd.* 511, (2012), 129

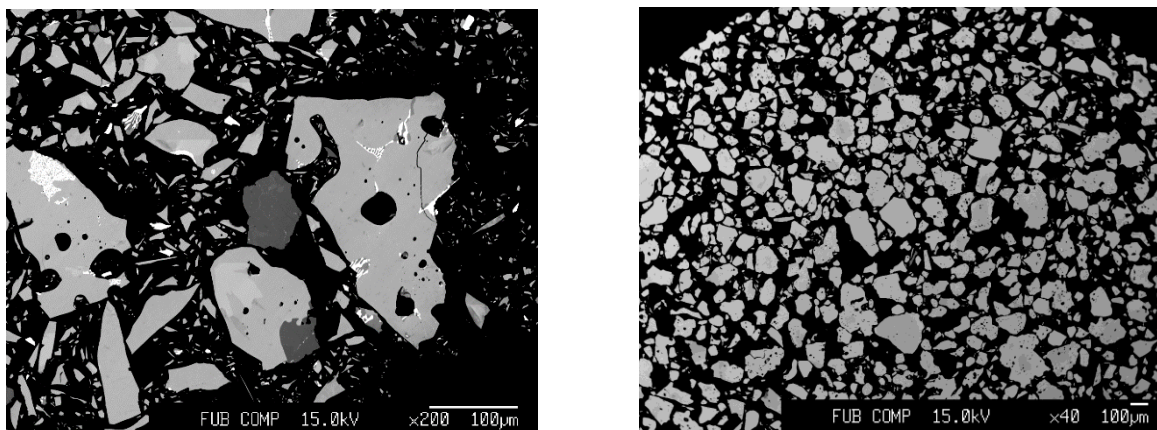


Figure 1 BSE micrograph of the samples $\text{Cu}_{1.92}\text{Zn}_{1.05}\text{Sn}_{0.99}\text{S}_{3.40}\text{Se}_{0.60}$ (a) and $\text{Cu}_2\text{ZnSnS}_{1.70}\text{Se}_{2.30}$ (b).

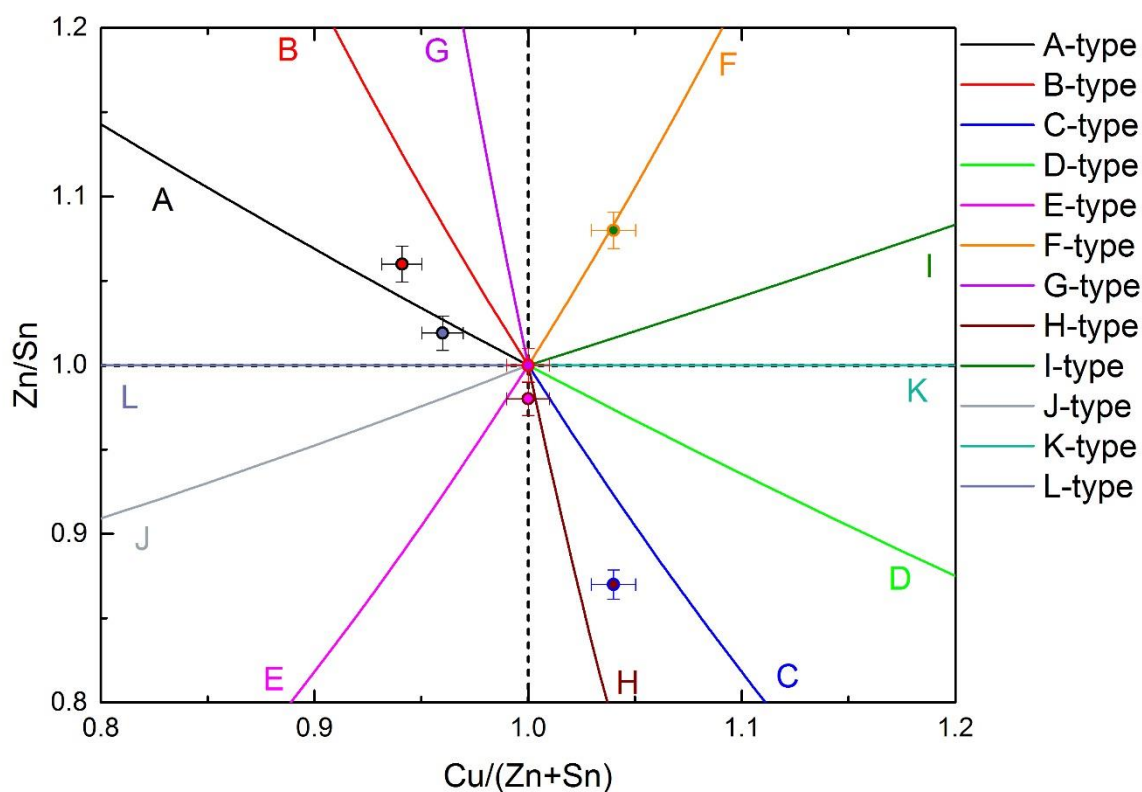


Figure 2. Cation ratio plot showing all CZTSSe mixed crystals synthesized. All of the stoichiometric Se-rich samples are located in the stoichiometric point at $\text{Cu}/(\text{Zn}+\text{Sn}) = \text{Zn}/\text{Sn} = 1$. The S-rich CZTSSe mixed crystals show an off-stoichiometric composition. The off-stoichiometry types refer to [13].

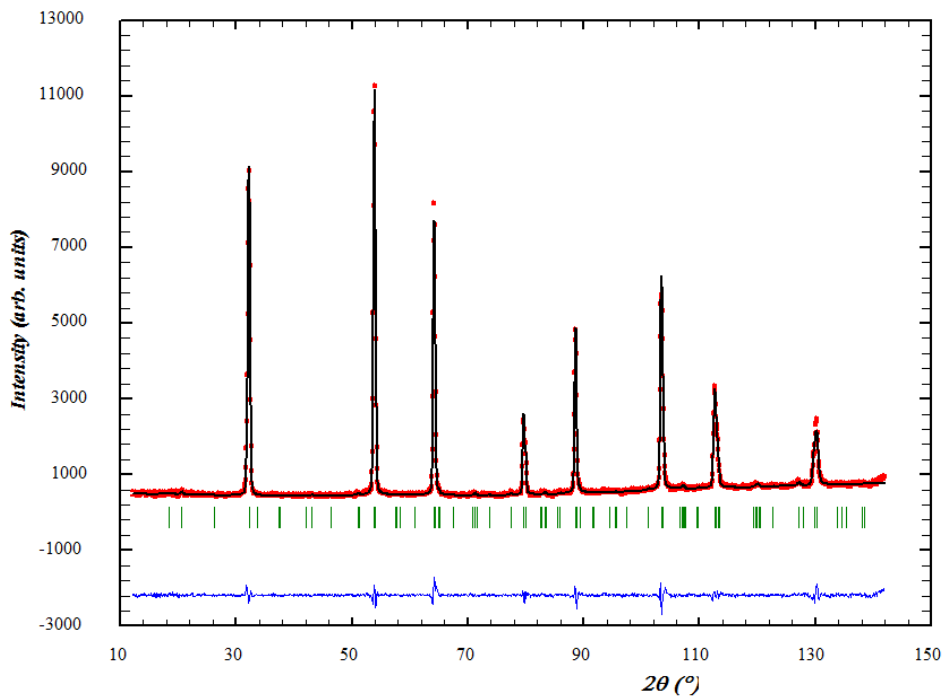


Figure 3. Exemplarily Rietveld analysis of a diffraction pattern collected at the Berlin Research Reactor (example: kesterite phase $\text{Cu}_2\text{ZnSnS}_{1.20}\text{Se}_{2.80}$ and no secondary phases). Red-observed pattern, black-calculated pattern and blue - difference line

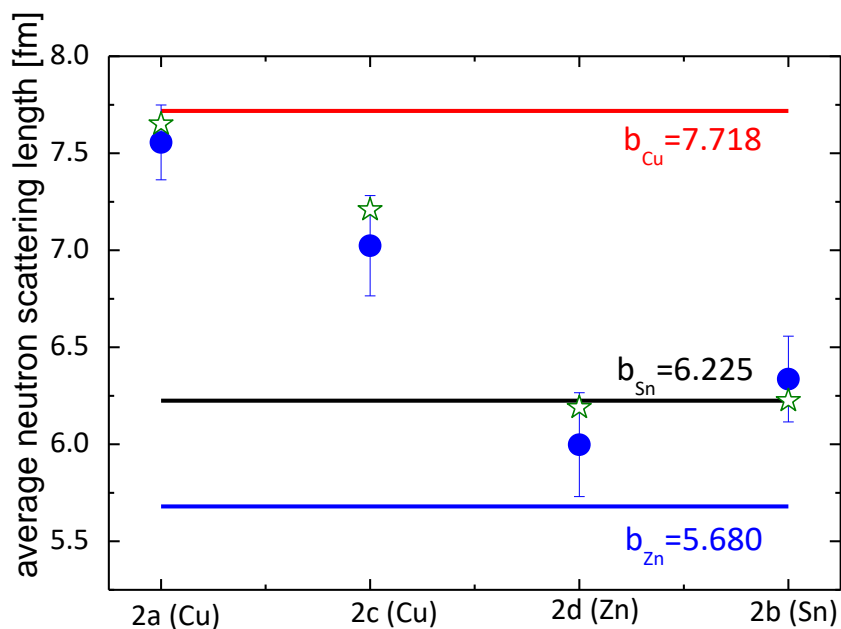


Figure 4 Average neutron scattering length \bar{b} of the cation sites $2a$, $2c$, $2d$ and $2b$ for $\text{Cu}_2\text{ZnSnS}_{0.84}\text{Se}_{3.16}$, (full symbols – experimental values; star – calculated values from best distribution model; lines – pure elements).

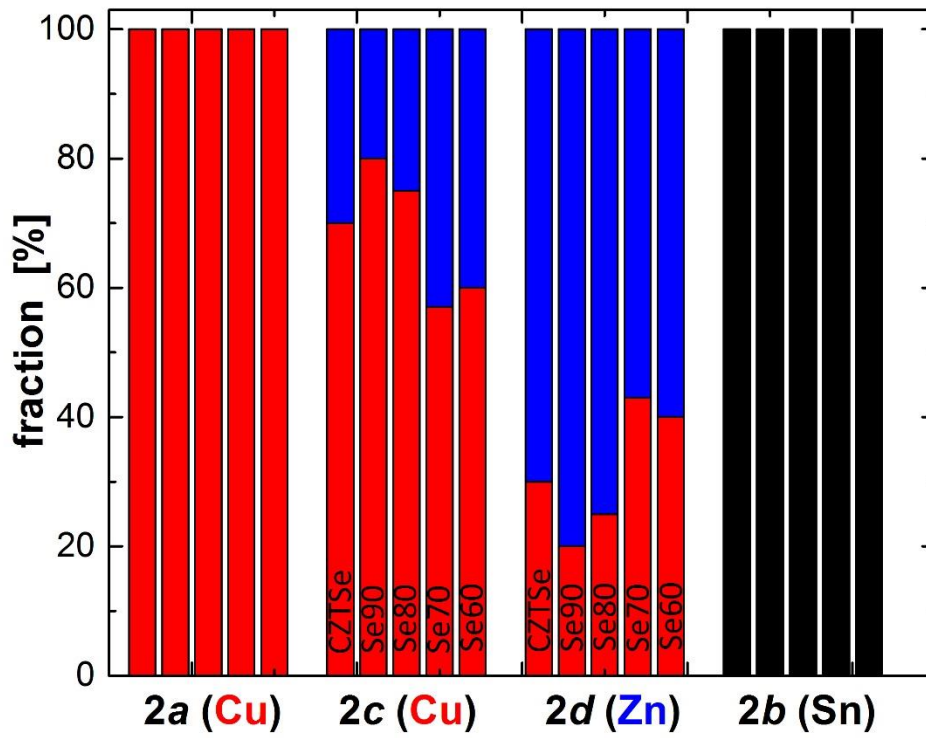


Figure 5 The resulting cation distribution on the structural sites *2a*, *2b*, *2c* and *2d* for all CZTSSe samples, obtained from the in-depth analysis of neutron diffraction data. Within the columns for one Wyckoff site the Se-content decreases from left to right.

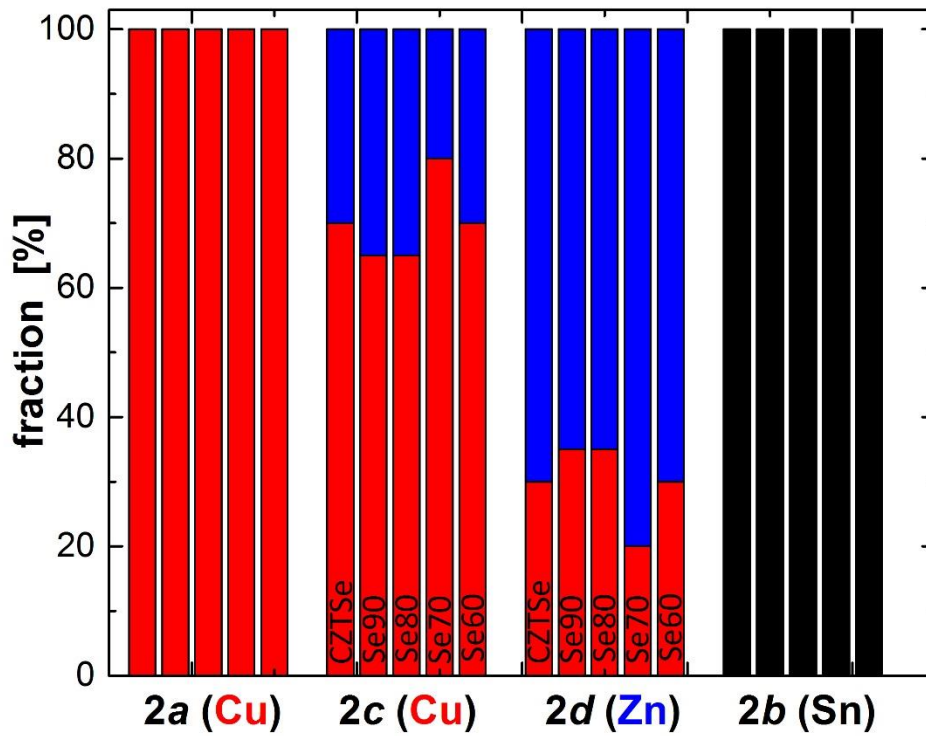


Figure 6. The resulting cation distribution on the structural sites 2a, 2b, 2c and 2d for all CZTSSe samples, obtained from the in-depth analysis of anomalous X-ray diffraction data. Within the columns for one Wyckoff site the Se-content decreases from left to right.

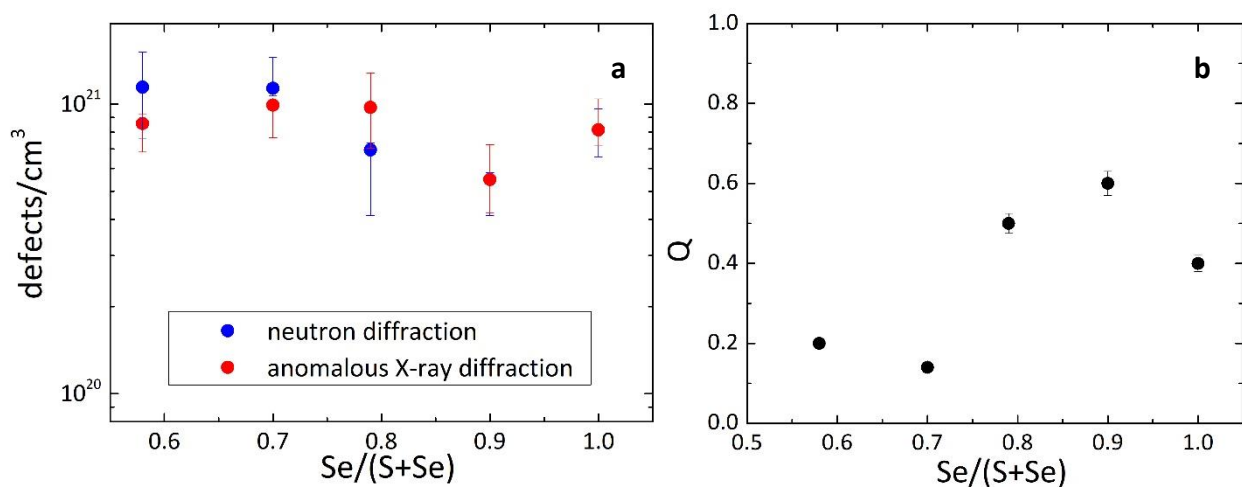


Figure 7. a) Concentration of Cu_{Zn} and Zn_{Cu} anti site defects (defects/cm³) representing Cu/Zn disorder obtained from neutron diffraction (blue dots) and anomalous X-ray diffraction (red dots) in Se-rich CZTSSe mixed crystals; b) the order parameter Q (black dots) calculated according to eq.2.

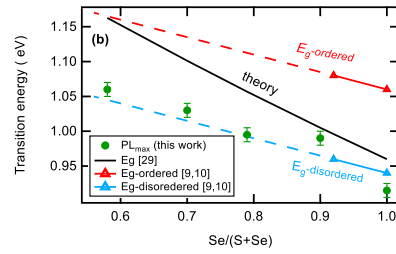
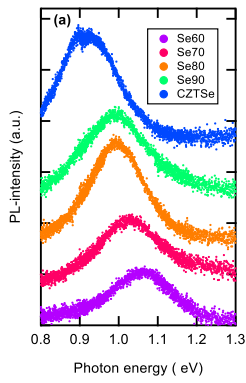


Figure 8. a) Photoluminescence spectra of the Se-rich CZTSSe mixed crystals with different Se/(S+Se) ratios; b) A comparison of the PL emission maximum energy (PL_{\max}) and reported values of the theoretically calculated band gap energy (black line) [29] and the band gap energy of “ordered” and “disordered” CZTSSe thin films [9, 10].

Table 1 Overview of the synthesized CZTSSe samples: cation ratios Cu/(Zn + Sn) and Zn/Sn of the CZTSSe phase obtained from the electron microprobe analysis (WDX spectroscopy), occurring secondary phases, final formulae of the kesterite-type phase and the off-stoichiometry types, in case of off-stoichiometric composition, are given.

Name	Cu/(Zn+Sn)	Zn/Sn	x=Se/(S+Se)	chemical formula	secondary phases	off-stoichiometry type
Se 10	1.04	1.08	0.09	$\text{Cu}_{2.13}\text{Zn}_{1.01}\text{Sn}_{0.96}\text{S}_{3.63}\text{Se}_{0.37}$	-	F-I
Se 20	0.94	1.06	0.15	$\text{Cu}_{1.92}\text{Zn}_{1.05}\text{Sn}_{0.99}\text{S}_{3.40}\text{Se}_{0.60}$	$\text{SnS}_{0.5}\text{Se}_{0.5}$ $\text{Cu}_2\text{S}_{0.7}\text{Se}_{0.3}$ ZnS	A-B
Se30	0.96	1.02	0.23	$\text{Cu}_{1.94}\text{Zn}_{1.02}\text{Sn}_{0.96}\text{S}_{3.08}\text{Se}_{0.92}$	$\text{SnS}_{0.5}\text{Se}_{0.5}$ ZnS	A-L
Se 50	1.04	0.87	0.48	$\text{Cu}_{2.02}\text{Zn}_{0.91}\text{Sn}_{1.04}\text{S}_{2.08}\text{Se}_{1.92}$	-	H-C
Se 60	1.00	0.98	0.58	$\text{Cu}_2\text{Zn}_{0.99}\text{Sn}_{1.01}\text{S}_{1.68}\text{Se}_{2.32}$	-	-
Se 70	1.00	1.00	0.70	$\text{Cu}_2\text{ZnSnS}_{1.20}\text{Se}_{2.80}$	-	-
Se 80	1.00	1.00	0.79	$\text{Cu}_2\text{ZnSnS}_{0.84}\text{Se}_{3.16}$	-	-
Se 90	1.00	1.00	0.90	$\text{Cu}_2\text{ZnSnS}_{0.40}\text{Se}_{3.60}$	-	-
CZTSe	1.00	1.00	1.00	$\text{Cu}_2\text{ZnSnSe}_4$	-	-

Table 2 Lattice parameters and site occupancy factors determined from neutron diffraction data.

Name	Lattice parameters		SOF			
	<i>a</i> , Å	<i>c</i> , Å	Cu 2 <i>a</i>	Cu 2 <i>c</i>	Zn 2 <i>d</i>	Sn 2 <i>b</i>
Se 50	5.550(1)	11.123(2)	0.945(35)	0.995(43)	1.167(49)	0.982(40)
Se 60	5.599(1)	11.159(2)	0.991(34)	0.895(56)	1.153(37)	1.000(40)
Se 70	5.616(1)	11.191(2)	1.017(40)	0.894(46)	1.196(57)	1.005(44)
Se 80	5.651(1)	11.261(2)	0.979(50)	0.912(47)	1.056(52)	1.010(44)
Se 90	5.676(1)	11.311(2)	1.010(28)	0.925(35)	1.037(44)	0.988(32)
CZTSe	5.693(1)	11.347(2)	0.964(35)	0.891(56)	1.117(50)	0.983(43)

Table 3 Cation distribution deduced from neutron and anomalous X-ray diffraction data analysis. Values represent fractions of cations occupying a structural site, with 1.00 a site is fully occupied. An error of 5% can be considered for all of these values.

Name	Neutron diffraction					Anomalous X-ray diffraction				
	<i>Cu</i> <i>2a</i>	<i>Cu</i> <i>2c</i>	<i>Zn</i> <i>2c</i>	<i>Cu</i> <i>2d</i>	<i>Zn</i> <i>2d</i>	<i>Cu</i> <i>2a</i>	<i>Cu</i> <i>2c</i>	<i>Zn</i> <i>2c</i>	<i>Cu</i> <i>2d</i>	<i>Zn</i> <i>2d</i>
Se 60	1.00	0.60	0.40	0.40	0.60	1.00	0.70	0.30	0.30	0.70
Se 70	1.00	0.57	0.43	0.43	0.57	1.00	0.65	0.35	0.35	0.65
Se 80	1.00	0.75	0.25	0.25	0.75	1.00	0.65	0.35	0.35	0.65
Se 90	1.00	0.80	0.20	0.20	0.80	1.00	0.80	0.20	0.20	0.80
CZTSe	1.00	0.70	0.30	0.30	0.70	1.00	0.70	0.30	0.30	0.70